

HIGH DUTY CYCLE ACTIVE SONAR USING BROADBAND DOPPLER-SENSITIVE WAVEFORMS: EXPLOITING A TRIPLET ARRAY FOR ATTENUATING DIRECT PATH INTERFERENCE

Michael Datum

General Dynamics Applied Physical Sciences Corp.
475 Bridge Street
Groton, CT 06340 USA
mdatum@aphysci.com

Abstract: *The class of active sonar waveforms that are Broadband and Doppler Sensitive (BBDS) is investigated for High Duty Cycle (HDC) sonar applications. BBDS waveforms include Pseudo Random Noise (PRN), Frequency Shift Keyed (FSK), and various phase modulated waveforms. The work here focuses on pseudo-random Minimum Shift Keyed (MSK) sequences, which provide good band constraint with efficient power levels, though much of the analysis applies to the entire class of waveforms. HDC sonar presents challenges for BBDS waveforms due to matched-filter sidelobe masking from the direct path. A technique is developed for suppressing the direct path as well its specular surface and bottom reflections, which exploits the properties of a triplet hydrophone array. Data from the Littoral Continuous Active Sonar 2015 (LCAS 15) experiment is analyzed, in which an echo repeater serves as the target.*

Keywords: *broadband waveforms, continuous active sonar, triplet array, high duty cycle sonar*

1. INTRODUCTION

Broadband Doppler sensitive waveforms

The continuous wave (CW) and frequency modulated (FM) waveforms are those most commonly used for active sonar. CW waveforms are sensitive to Doppler, but poor at resolving range, while FM waveforms resolve range well but are not sensitive to Doppler. Broadband Doppler sensitive (BBDS) waveforms can resolve both range and Doppler simultaneously, but typically suffer from matched filter sidelobes. BBDS waveforms include frequency shift keyed (FSK), which are often transmitted in a Costa's sequence [1], and various phase based methods, such as binary phase-shift keyed (BPSK) [2]. The BBDS waveform we analyze here is the minimum shift keyed (MSK) waveform, though the processing described can apply to any BBDS waveform.

MSK signalling, sometimes also called continuous phase frequency shift keying (CPFSK), was developed for digital communications. It employs both phase and frequency shift over many sub-pulses. In conventional MSK, the signal is encoded as two frequencies, f and $1.5f$, so that if the frequency is shifted from f to $1.5f$ or vice versa, the phase can be shifted by 180° (by multiplying by -1) if needed in order to maintain constant phase over the transition. The constant phase results in less spectral spread of the signal, while maintaining constant amplitude. Here we modify the MSK to allow arbitrary frequency choices for the two sub-pulse frequencies, which requires the phase to be computed at each transition to maintain constant phase. For a digital communications encryption, this would make decoding difficult, but here we need only maintain the transmit signal for matched filtering.

The MSK with bandwidth B , pulse length T , and center frequency f_0 is then generated as a sequence of sub-pulses, $\mathbf{s} = [\mathbf{s}_1 \mathbf{s}_2 \dots]$, each of duration $T_{sub} = 1/B$, computed by

$$s_k(n) = \cos \left[\frac{j2\pi f_k n}{f_s} + \phi_{k-1} \right] \quad n = 0, 1, \dots, [f_s T_{sub}] - 1, \quad k = 1, 2, \dots, \left\lceil \frac{T}{T_{sub}} \right\rceil \quad (1)$$

Since the sub-pulse length results in sub-pulse bandwidth of $1/T_{sub}$, we choose the two frequencies to fill the band, and the phases for each sub-pulse to maintain constant phase,

$$f_k = \begin{cases} f_0 - \frac{B}{4} & \text{if } u_k = 0 \\ f_0 + \frac{B}{4} & \text{if } u_k = 1 \end{cases} \quad \phi_k = \text{mod}[2\pi T_{sub} f_k + \phi_{k-1}, 2\pi] \quad (2)$$

Where u_k randomly chosen with $P\{u_k = 0\} = P\{u_k = 1\} = 0.5$. In digital communications, the MSK is typically filtered with a Gaussian filter, which has zero overshoot step response. Here we filter with a more aggressive forward-backward (zero-phase) second order Butterworth filter to reduce spectral leakage at the expense of waveform extrema that reduces the RMS-to-peak ratio by about 1 dB.

Searching for an acoustic echo with Doppler sensitive waveforms entails matched filtering with a portion of the transmitted waveform that has been dilated in time to represent varying possible Dopplers of the echo. The ideal matched filter response can be characterized by the wideband ambiguity function (WAF) across varying time lag, τ , and Doppler, or range rate, \dot{r} ,

$$\Psi(\tau, \alpha) = \sqrt{\alpha} \int_{-\infty}^{\infty} s(t) s^*[\alpha(t - \tau)] dt, \quad \alpha = \frac{c + \dot{r}}{c - \dot{r}}, \quad c \equiv \text{sound speed} \quad (3)$$

The WAF for an 18 second filtered MSK with bandwidth 800 Hz and center frequency 2200 Hz, matched filtered with the full waveform is plotted in Figure 1, with power vs. range at zero Doppler, and maximum power across Doppler also plotted. Sidelobes, which have root-mean-square value a factor $T \cdot B$ lower than the peak, are evident. The lower right plot shows a close-

up of the main-lobe, which has range resolution of $\frac{c}{2B} \cong 0.5 \text{ m}$ and Doppler resolution of $\frac{c}{Tf_0} \cong 0.02 \text{ kts}$. Note that processing with only a portion of the waveform will reduce both range and Doppler resolution, while increasing sidelobe energy.

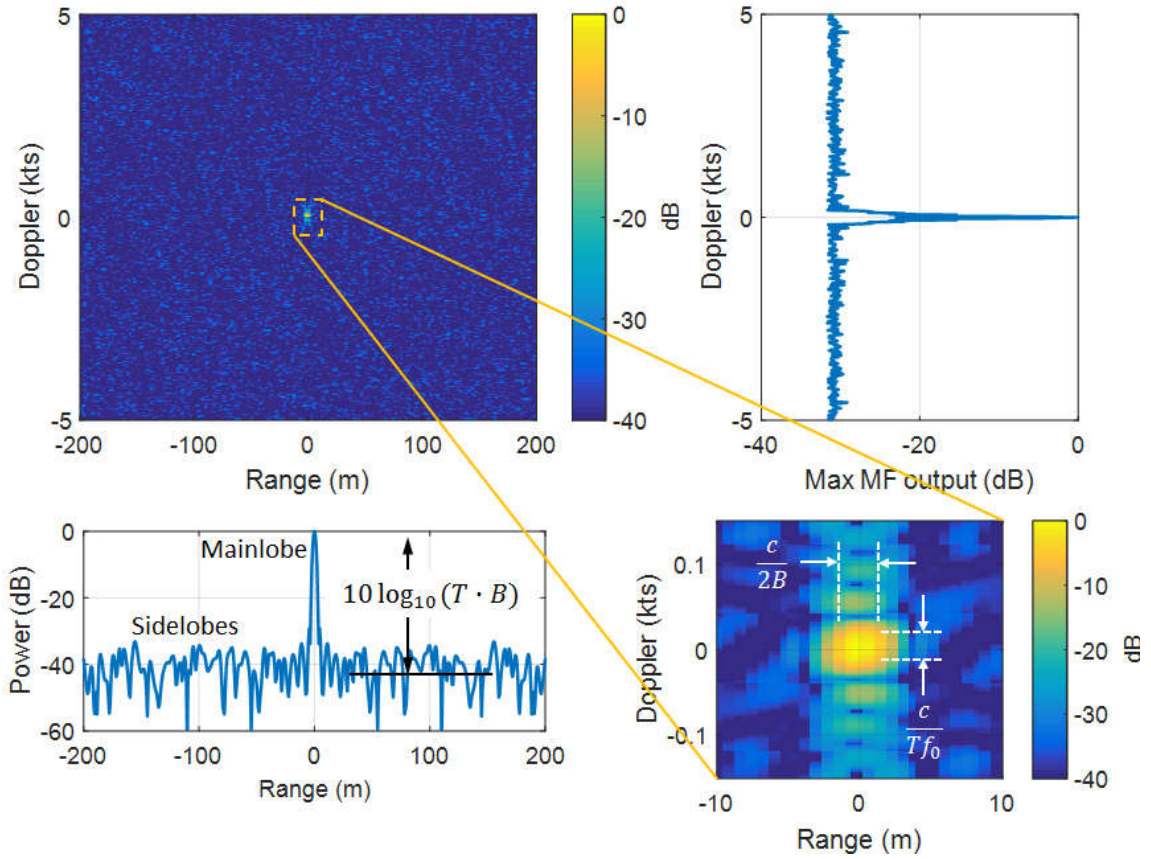


Figure 1: WAF for the filtered MSK across range and Doppler (upper left), the WAF power at zero Doppler (lower left), maximum WAF power over all range (upper right), and close-up of the main-lobe (lower right).

High duty cycle sonar and broadband Doppler sensitive waveforms

In high duty cycle (HDC) sonar, the probing transmit pulse is retransmitted at a rate such that matched filter search interval and transmit interval may overlap. Continuous active sonar (CAS) is a type of HDC sonar in which the transmit signal is repeated without delay. Figure 2 shows the post-beamformer spectrogram and matched filter output for both a LFM and MSK pulse, transmitted in shallow water with echo-repeater serving as target. For both waveforms, the repetition interval is 20 sec, with $T = 18 \text{ sec}$ and $B = 800 \text{ Hz}$. The LFM spectrogram shows how the direct path transmission is still being received when the target echo first arrives. Although the data is beamformed, the off-axis beam response is high enough that the direct path energy is still significant.

The right half of Figure 2 depicts the primary difficulty with using BBDS waveforms for HDC sonar. The significant sidelobes for the MSK, about $10 \log_{10}(TB)$ down from the peak, appear as noise-like and mask the typically much weaker target echo. In this example, the sidelobes would need to be reduced by about 30 dB to yield even a 10 dB signal to noise ratio (SNR), where “noise” is here the sidelobes. Moreover, the specular surface and bottom bounce energy from the source can arrive at much steeper angles. If a hydrophone line array is used, the conical beam shape can result in this strong bottom or surface reflection energy appearing in the near broadside beams typically where the primary target search is performed.

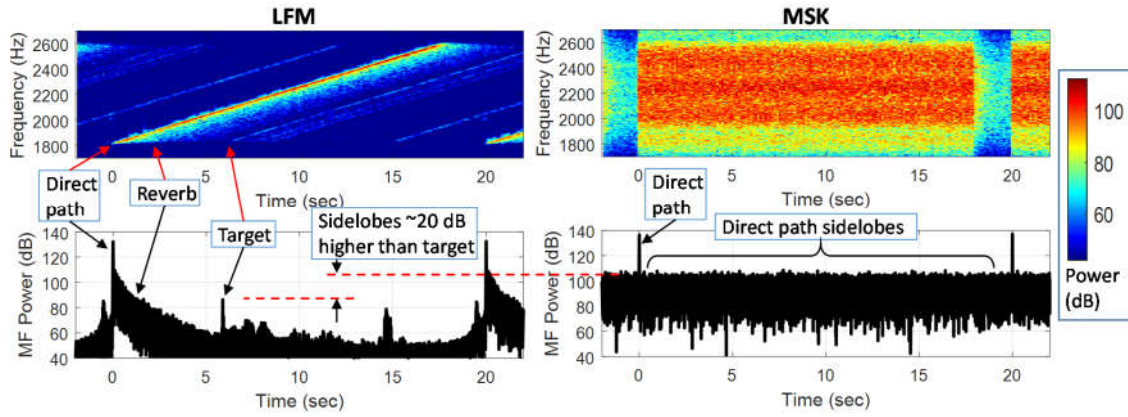


Figure 2: Example spectrograms (top) and zero Doppler matched filtered output (bottom) for both LFM (left), and MSK HDC (right) waveforms, with $T=18$ sec, $B=800$ Hz, repeated every 20 sec. In the LFM matched filter plot, the direct path, reverb, and target echo are clearly visible, while the matched filter sidelobes from the MSK direct path mask the target echo.

2. REDUCING DIRECT PATH INTERFERENCE

Reducing the strong direct path interference described above can be done by modifying the transmit waveform, by using temporal based techniques, or by exploiting spatial differences between the direct path and the desired search space. Modifying the waveform is currently being investigated by this and other authors [3], but will not be discussed here. Previous work in temporal based methods, sometimes called adaptive matched filtering, e.g. [4,5] have shown promise, but can be computationally expensive. Current research by the author includes implementation of the CLEAN algorithm [6], which requires less computation and has shown good results. Spatial based techniques include adaptive beamforming and adaptive noise cancellation, and will be the focus of this paper.

Spatial based methods of direct path interference reduction can be limited by spatial overlap of the interference and search space (as described above), by unknown spatial diversity of the target, and by temporal variation of the received signal in active sonar applications. We will begin with conventional and adaptive beamforming, and introduce a technique that takes advantage of properties of a triplet line array and the directivity of the primary source-to-receiver acoustic paths that make up the bulk of the interference.

Beamforming for interference rejection

Defining the steering vector $\mathbf{d}(k)$ as the set of complex phase terms at frequency bin k for aligning data from all hydrophones coming from a single beam direction, and defining the hydrophone data vector as $\mathbf{x}(k)$, the beam output of a conventional beamformer is computed as the projection of the data onto the desired steering vector, (suppressing the frequency bin index k),

$$y = \mathbf{d}^T \mathbf{x} \quad (4)$$

By shading the steering vector, the beam sidelobes of a conventional beamformer can be reduced significantly, but at the expense of a larger beam mainlobe, which can result in increased reverberation in the beam.

Adaptive beamforming methods sample the data over time and use the information to improve the beamforming, typically suppressing directional interferences. The Minimum Variance Distortionless Response (MVDR) beamformer estimates the steering vector by

$$\mathbf{w} = \frac{\mathbf{R}^{-1}\mathbf{d}}{\mathbf{d}^T \mathbf{R}^{-1} \mathbf{d}} \quad (5)$$

where $\mathbf{R} = E\{\mathbf{xx}^T\}$ is the Cross Spectral Density Matrix (CSDM). The MVDR beamformer results in nulls steered towards any strong interferers, unless they are in the direction of the steering vector, which is always unit gain. Estimating \mathbf{R} is typically done by averaging the data. Since the MSK waveform is continuously full-band, the estimate can be made over a portion of a ping, whereas for waveforms that vary over time, such as the LFM, multiple pings may be necessary to get a full-rank estimate.

For a horizontal triplet (or cardioid) array, which is a line array consisting of sets of hydrophones arranged in closely spaced equilateral triangles, the processing is typically designed to form a cardioid using each set with null steered to the side opposite the look direction [7]. This is used to disambiguate targets on the port or starboard sides of the array. Here processing is presented that instead uses the triplets to attenuate the direct source-to-receiver path interference as well as the specular surface and bottom bounce reflections, at the expense of now having no port-starboard ambiguity resolution.

It is first noted that the direct and specular surface/bottom reflected paths are largely confined to the vertical plane connecting the source and the midline of the array, as depicted in Figure 3. Also shown in the figure are several dipoles, which can be formed using the hydrophone triplets. The dipoles can be oriented such that their nulls are oriented on the direct and surface/bottom reflection interference plane. The properly calibrated dipole outputs can then be beamformed as a line array.

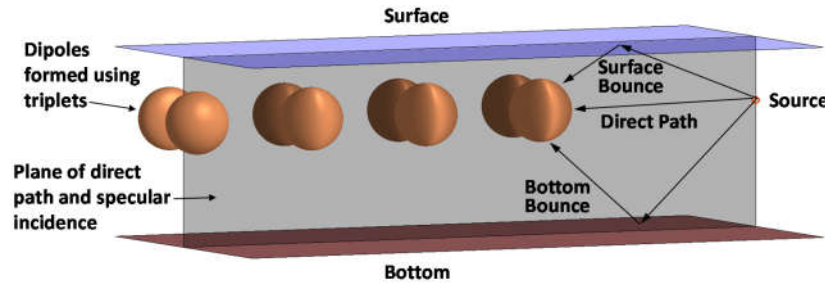


Figure 3: Illustration of direct and surface/bottom specular reflected interference, which are primarily directed along the vertical plane connecting the source and sensors. The hydrophone triplets can be used to form dipoles with nulls oriented on that same plane.

Formation of a dipole using a pair of closely spaced hydrophones can be achieved by differencing the two and scaling by the expected attenuation at the maximum response axis (MRA) of the dipole. Likewise, an orthogonally oriented dipole can be formed using the third hydrophone in the triplet and a scaled sum of the first two. The equations for generating the dipoles, with proper calibration for frequency f_0 , are

$$d_1(t) = \frac{x_2(t) - x_3(t)}{2\sin(\pi f_0 s/c)} \quad d_2(t) = \frac{x_1(t) - [x_2(t) + x_3(t)]/2\cos(\frac{\pi f_0 s}{c})}{2\sin(\pi f_0 \sqrt{3}s/2c)} \quad (6)$$

where d_1 and d_2 are the horizontally and vertically oriented dipoles, respectively, and x_1 , x_2 , and x_3 are the three hydrophones in a single triplet with spacing s between hydrophones. The equations in (6) result in dipoles with centers offset by $\frac{\sqrt{3}}{4}s$, as illustrated in Figure 4. This will be negligible in terms of amplitude differences at target ranges, but will result in elevation dependent phase offset that will affect subsequent beamforming of the dipole data.

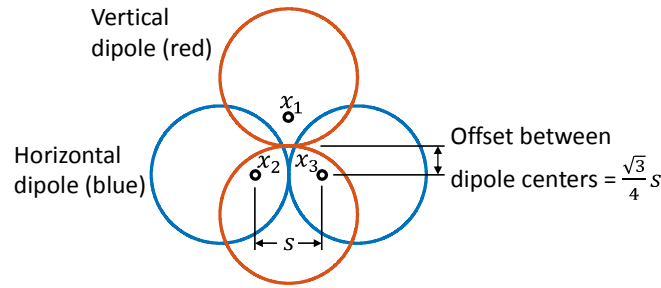


Figure 4: Illustration of the horizontal and vertical dipoles formed using the equations in (6).

The two dipoles can be closely approximated by $d_1 = \cos(\phi)$, $d_2 = \sin(\phi)$ where ϕ is the elevation on the plane perpendicular to the array centreline. To correct for possible roll of the array triplets, the dipoles are combined using the identity

$$d_\rho = \cos(\phi + \rho) = d_1 \cos(\rho) + d_2 \sin(\rho) \quad (7)$$

where ρ is the roll angle of the triplet, and d_ρ is the roll-corrected dipole.

3. EXPERIMENTAL RESULTS

The Littoral Continuous Active Sonar 2015 (LCAS 15) experiment was performed by an international team led by the NATO Centre for Maritime Research and Experimentation (CMRE). It took place off La Spezia, Italy in October 2015 where the bottom depth was upslope towards the target from 110 to 60 m. Both MSK and LFM waveforms were transmitted with the same pulse duration, 18 sec, and bandwidth, 800 Hz, centered at 2200 Hz, in similar geometries. The active source was towed about 150 m forward of the Five Octave Research Array (FORA), which had a set of 78 hydrophone triplets. An echo-repeater served as target, and was towed in the opposite direction at a closest point of approach of about 4500 m.

Both the LFM and MSK hydrophone data were processed to form dipoles using the equations in (6), and the measured roll of the array was used to rotate the dipole using equation (7) such that the dipole nulls were oriented vertically. To test the ability of the dipole technique to suppress the direct path and surface/bottom specular interference, the LFM results are first analyzed, with the matched filter output plotted on the lower left half of Figure 5 for both a single hydrophone (red) and a single dipole (black). The close-up around the direct path is plotted on the top, where it can be seen that the dipole direct path peak and surface/bottom specular energy, which is less than 100 m after the peak, are decreased by about 20 dB lower than the single hydrophone. The MSK waveform data was matched filtered, with the zero Doppler outputs plotted in the lower right of Figure 5. The target was expected to be at zero Doppler. Again the direct path peak for the dipole is about 20 dB lower than the single hydrophone, but it can be seen that the sidelobes are also decreased by 20 dB. The LFM energy near the target is decreased somewhat because the dipole is rejecting reverberation and ambient noise, but there are no significant sidelobes with the LFM. The target peak for the LFM is decreased by about 1 dB, possibly because the energy is not arriving in at the center of the dipole in the vertical direction. The target in the MSK case is still masked by the sidelobes from the direct path.

The MVDR beamformer described in equation (5) was applied to the 78 dipole outputs, treated as a line array, with the beam steered in the known direction of the target (near broadside). A MVDR Beamformer was also applied to all 234 hydrophones of the full volumetric array as comparison, this time with the beam steered towards the target in azimuth, but at zero elevation. Both MVDR Beamformer results are plotted in Figure 6, for both the LFM waveform (left) and MSK (right). Both MVDR beamformers suppressed the direct path

about 50 dB lower than the single dipole, and the surface/bottom specular energy by about 20 dB. The full volumetric MVDR also suppressed the target echo by about 20 dB. The MSK waveform dipole MVDR beamformed direct path was suppressed by over 50 dB, but two peaks occurred near where the direct path was. The sidelobe energy only decreased by about 30 dB from the single dipole. The full MVDR beamformer had similar multiple peaks, but the sidelobes were decreased by about 50 dB. The target was likely also suppressed for this case.

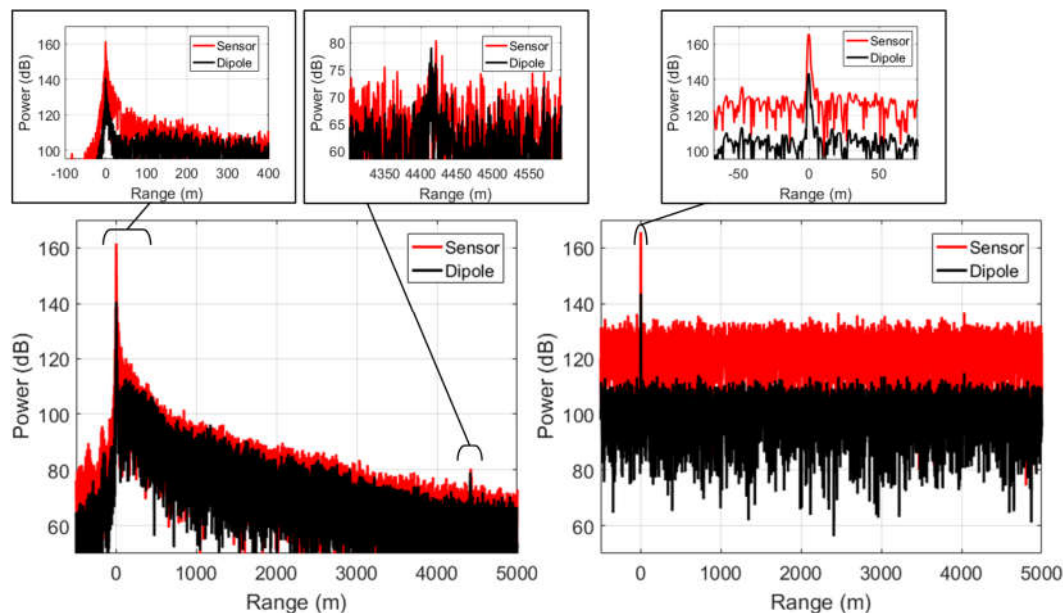


Figure 5: LFM (lower left) and MSK (lower right) matched filter outputs for single hydrophone (red) and a single dipole (black). Top plots show close-ups around the direct path and target peaks for the LFM and the direct path peak for the MSK. For both waveforms, the direct path and surface/bottom interaction (less than 100 m range) are suppressed by about 20 dB. The MSK shows a similar decrease in the sidelobes.

4. CONCLUSIONS

A method for reducing the direct path and the surface and bottom specular reflected interference in HDC sonar was introduced and experimentally demonstrated. The technique, which exploits the properties of a triplet hydrophone array, forms a set of orthogonal dipoles and steers them to form a null along the vertical plane where the direct and specular bounce paths are prevalent. The resulting set of steered dipoles were then beamformed as a line array. Since the steered dipoles were formed from dipoles with different phase centers, they had phase shift dependent on the roll correction and the arrival angle of the interference. A MVDR beamformer was used, since it estimates the phase of the strong interfering energy and steers nulls in those directions.

Results from the LCAS 15 experiment were analysed to test the algorithm, where both LFM and MSK HDC waveforms were transmitted. The LFM, which didn't suffer from matched filter sidelobe masking, allowed the effect on direct and specular paths and the target to be observed. About 20 dB of direct and specular interference suppression was seen for the individual dipoles, with only about 1 dB of target level decrease. For the dipole MVDR, there was about 50 dB of additional suppression of the direct path, and 30 dB of the specular, with about 1 dB more of target level decrease. The MSK signal, which had significant matched filter sidelobe masking, showed a decrease in direct path, and associated sidelobes, of about 20 dB for the dipole, and about 25 dB more decrease for the MVDR sidelobe levels.

A full volumetric MVDR beamformer was also implemented for comparison, which again showed significant reduction in the direct and specular paths, but also a significant reduction in

the target level. This is possibly because the target acoustic path did not arrive at zero elevation where the elevation of the full volumetric MVDR was, and was cancelled by the beamformer.

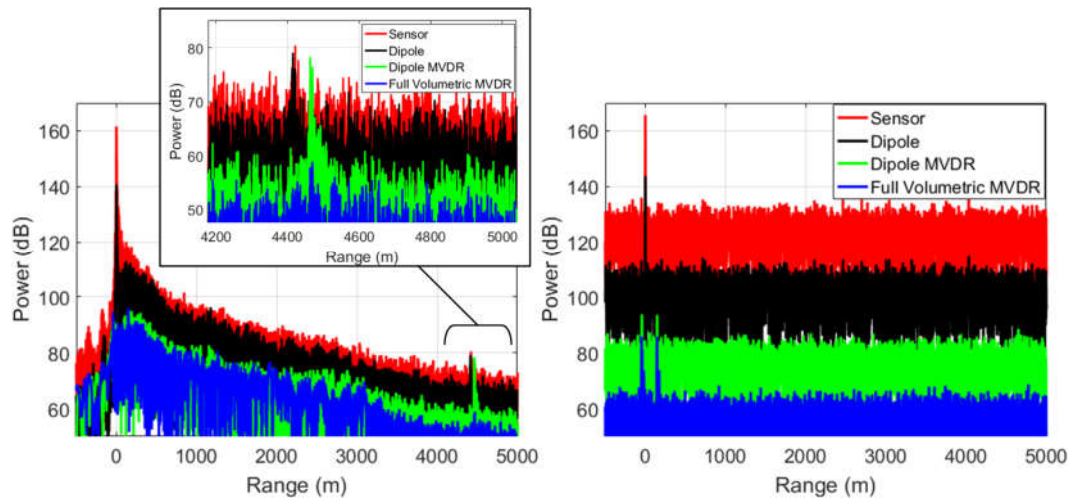


Figure 6: MVDR beamformer applied to the 78 dipoles after matched filtering (green) and a full volumetric MVDR beamforming applied to all 234 hydrophones (blue), for both the LFM waveform (lower left) and the MSK (lower right). Note that both the full volumetric and dipole beamformers suppresses the direct path interference well, but the full volumetric also suppresses the target. The LFM waveform sidelobes are suppressed, but still higher than the expected target level. The original single hydrophone and dipole are also plotted.

ACKNOWLEDGEMENTS

This work was funded by the Office of Naval Research Code 321. The LCAS 15 experiment could not have been possible without the efforts of NATO CMRE and the test participants.

REFERENCES

- [1] **Costas, J. P.**, A study of a class of detection waveforms having nearly ideal range-Doppler ambiguity properties, *Proceedings of the IEEE*, 72 (8), pp. 996–1009, 1984.
- [2] **Mathieu, E. and S. Beerens**, False-alarm reduction for low-frequency active sonar with BPSK pulses: Experimental results, *IEEE Journal of Oceanic Engineering*, 36 (1), pp. 53–60, 2011.
- [3] **Hague, D. and J. Buck**, The generalized sinusoidal frequency-modulated waveform for active sonar, *IEEE Journal of Oceanic Engineering*, 42 (1), pp. 109–123, 2017.
- [4] **Ling, J., Li, J., Stoica, P., and Datum, M.**, On probing waveforms and adaptive receivers for active sonar, *Journal of the Acoustical Society of America*, 129 (6), pp. 3640–51, 2011.
- [5] **Lourey, S.**, Adaptive filtering for enhanced detection of continuous active sonar signals, In *4th Underwater Acoustics Conference and Exhibition*, Skiathos, Greece, ed. by John Papadakis, pp. 145–152, 2017.
- [6] **Högbom, J.**, Aperture synthesis with a nonregular distribution of interferometer baselines, *Astron. Astrophys. Supplements*, vol. 15, pp. 417–426, 1974.
- [7] **Baldacci, A., Haralabus, G., and van Velzen, M.**, Cardioid receive array calibration for active systems, *NATO Undersea Research Centre Technical Report NURC-PR-2006-015*, 2006.